

Original Research

A New Method for the Determination of Tellurium Using Slotted Quartz Tube-Flame Atomic Absorption Spectrophotometry with Modified Magnetic Nanoparticles

Fatma Ötünç^{1*}, Berrin Ziyadanoğulları², Fırat Aydın²

¹Dicle University Institute of Science and Technology Diyarbakır Turkey

²Dicle University Faculty of Science Diyarbakır Turkey

Received: 5 February 2025

Accepted: 2 June 2025

Abstract

Toxic metals have the ability to accumulate in the human body over time, leading to chronic exposure and serious health complications. Tellurium (Te), the heaviest stable chalcogen, is a rare element in the Earth's crust and is considered toxic even at low concentrations. Prolonged exposure may damage the kidneys, liver, and nervous system.

In this study, a novel method was developed for the determination of trace amounts of Te(IV) using oleic acid-coated iron oxide magnetic nanoparticles (OAMNPs) for preconcentration, combined with slotted quartz tube-flame atomic absorption spectrometry (SQT-FAAS). The method was optimized for several parameters: buffer volume (1 mL), nanoparticle amount (50 mg), pH (8.0), contact time (60 seconds), and manual shaking time (120 seconds).

The developed method achieved a limit of detection (LOD) of 0.02 µg/L and a limit of quantification (LOQ) of 0.07 µg/L, with a preconcentration factor of 76.2. Matrix effects were investigated, and recovery studies demonstrated the method's high accuracy and applicability in real samples. The results confirmed that this approach is efficient, sensitive, and reliable for determining tellurium, even in complex matrices like cold tea.

Keywords: magnetic nanoparticles, microextraction, atomic absorption spectrometry, tellurium

Introduction

Toxic metals, which can be effective even at low concentrations, enter the organism through the mouth,

respiration, and skin and are generally not sufficiently removed by the body's excretion mechanisms (kidney, liver, intestine, lung, and skin). The accumulation of these metals in living things leads to increased concentrations, and when they reach a certain level, they can cause serious health problems (such as thyroid diseases, neurological disorders, autism, and infertility) and eventually death. [1]. Toxic element pollution of

*e-mail: fatmatnc1988@gmail.com

Tel.: +90 541 672 0325

°ORCID iD: 0009-0007-5009-1616

the environment due to human achievements has recently garnered much interest [2]. Metals accumulate in living things through the food chain, posing a risk in terms of toxicity and human exposure [3].

Tellurium (Te) is a metalloid with important applications in metallurgy, but its accumulation in nature poses environmental risks due to toxicity at low concentrations, affecting organs like the heart and kidneys. Common detection methods for monitoring environmental effects include flame atomic absorption spectrophotometry (FAAS) [4], inductively coupled plasma-optical emission spectrometry (ICP-OES) [5], and inductively coupled plasma-mass spectrometry (ICP-MS) [6]. FAAS is cost-effective but less sensitive; this limitation can be reduced by preconcentration techniques such as dispersive solid phase extraction (DSPE). Recent research has focused on various sorbents, including magnetic hydrogels, for extracting tellurium from water samples, followed by detection with SQT-integrated FAAS [7].

This study summarizes research in which two different analysis methods (Dowex and XAD systems) are examined and compared to determine tellurium, the raw material of CdTe PV modules used in solar energy production. The fact that CdTe is a rare element raises concerns that it may negatively affect module production in the long term. By comparing both systems' properties and analysis efficiencies, the research provides important findings that will contribute to developing effective methods for tellurium determination and future studies [8].

This effectively demonstrates the potential of tellurium to optimize the sulfur content of industrial steels. The research has addressed the microstructure, mechanical properties, fatigue performance, machinability, and corrosion resistance of tellurium steels in existing environments. The results show that tellurium-treated steels increase sulfur separation and mechanical properties. Additionally, tellurium improved the machinability of steels and improved fatigue recovery. However, there is no obvious effect on tellurium's tensile strength and fracture resistance. Research determines recommended tellurium properties for medium carbon micro-alloy steels [9].

Significant advances in tellurium-containing polymers have occurred in the last decade. These polymers are as important as other heteroatom-containing polymers due to their unique properties and potential for various applications. This review will examine the tellurium-containing polymers' diversity, synthesis methods, properties, and application areas [10].

An effective and simple method is proposed for the selective separation and recovery of tellurium and bismuth in an acidic leaching solution. This method reduces tellurium by 99.83% with Na_2SO_3 ; the crude tellurium degree is increased to 93.78%. The bismuth in the reduced solution can then be converted to 92.35% crude bismuth using 99.39% Fe powder. The proposed

method offers an effective approach for efficiently separating and recovering tellurium and bismuth [11].

In the study, it is stated that the manganese-oxidizing bacterium *Bacillus* sp. carries out Te0 oxidation, and this process reveals a new transformation mechanism. The bacterium has the ability to both oxidize Mn(II) and reduce Te(IV). When interacting with Mn^{2+} and Te^{4+} , manganese oxides (BioMnOx) and elemental tellurium, respectively, can be produced. This study highlights the need to reconsider tellurium species's environmental fate and ecological risks mediated by manganese-oxidizing bacteria. [12].

With this success, a new magnetic polymer, $\text{Fe}_3\text{O}_4@ \text{SiO}_2@ \text{PoPD}$, was synthesized to describe defects in water samples. Various characterization methods examined Te synthesized nanoparticles' morphology, formation, and magnetic properties. Under optimum uniform conditions, the linear range and detection region of the methods were determined. The method's success was determined in the analyses performed on real samples [13].

A different study was conducted to obtain tellurium and high-purity bismuth from processing zinc anode slime residue. By determining the appropriate sulfation roasting and leaching conditions, tellurium and bismuth were separated, and the recovery rates were determined as 84.9% and 97.1% [14].

Tellurium was purified for the first time by plasma-assisted chemical transport reaction and thermal decomposition. This method involves the interaction of hydrogen and tellurium vapors at low pressure. The behavior of metal and carbon impurities was studied. The method's effectiveness was demonstrated by preparing As_2Te_3 films and their analysis by mass spectrometry [15].

There is limited information on the intestinal absorption and metabolic behavior of tellurium in humans. Studies in which different forms of tellurium were administered to healthy male volunteers found that soluble tellurium salts had 25% intestinal absorption, with tetravalent tellurium being excreted more rapidly than the hexavalent form. Tellurium in cress had a 15% absorption rate, while metallic tellurium had a 10% absorption rate [16].

The selective metallization technique is promising for flexible electronics in roll-to-roll production but sputtered materials present difficulties. This study demonstrates large-scale production by overcoming these problems by sputtering Bi-Sb-Te and evaporating Ag or Cu. Thin films deposited at room temperature exhibit improved thermoelectric performance, while metal doping facilitates the transition from n-type to p-type. Plasma treatment eliminates the surface effects caused by metal evaporation, enabling the successful use of thermoelectric devices in wearable applications [17].

The lack of platinum (Pt)-based high-efficiency catalysts is a major problem for direct formic acid fuel cells (DFAFCs). This study developed Pt-PtTe₂

heterophase nanotrepang (HPNT) doped with a rare earth element (Y). Y doping improved the FAOR kinetics and provided a much higher activity and power density than the commercial Pt/C. These findings highlight the role of rare earth metals in developing more efficient Pt-based catalysts for DFAFCs [18].

This study investigated the efficient recovery of tellurium and gold from complex copper anode slurry (CCAS). Through chlorinated leaching mechanisms and thermodynamic analysis, the optimum leaching efficiencies of tellurium and gold reached 97.9% and 99.9%, respectively. Gold was adsorbed with high selectivity by sulfonated tri-*n*-octylamine-modified corncob, while copper powder effectively precipitated tellurium. The overall recovery rates were 91.85% for tellurium and 99.38% for gold, which has great potential for industrial applicability [19].

A study of 2,592 people in Japan showed that urinary tellurium levels were associated with blood pressure and hypertension. Grains, beans, vegetables, and fruits were identified as the main dietary sources of tellurium exposure. Experiments in mice showed that tellurium exposure increased blood pressure, which returned to normal when exposure was stopped. These findings provided the first evidence that tellurium exposure may be a universal risk factor for hypertension [20].

Silybin (SIB) is a drug with hepatoprotective effects but limited efficacy due to low oral bioavailability and extensive metabolism. In this study, solid lipid nanoparticles (SLN-SIB) and polymeric nanoparticles (PN-SIB) were used to improve the distribution of SIB, and solid lipid nanoparticles containing ursodeoxycholic acid (SLN-SIB-U) were also evaluated. These nanoparticle systems aim to increase the bioavailability of SIB [21].

The ionic gelation method synthesized chitosan nanoparticles (CS-NPs) and searched for medical applications such as drug delivery. CS-NPs prepared at 0.25% to 1.0% w/v concentrations were functionalized with polyethylene oxide (PEO) and PEO-polypropylene glycol (PPG). TEM analyses showed that the nanoparticles were between 11.3-14.8 nm in size and had a semi-crystalline structure. Functionalization with PEO-PPG increased crystallinity, and adding TPP strengthened hydrogen bonds. These findings revealed that the structural properties of CS-NPs changed depending on concentration and functionalization, increasing their potential for use in areas such as drug delivery [22].

In our study, a new analytical method was developed for analyzing tellurium at low limits utilizing OAMNP. To our knowledge, this is the first study in the literature to use OAMNP as an extraction medium to preconcentrate tellurium prior to determination in the SQT-FAAS system.

Materials and Methods

Chemicals and Reagents

A stock tellurium solution (1000 mg/L) was purchased from CPAchem and was used to prepare standard solutions by appropriate dilution with ultrapure water. Buffer solutions with pH values ranging from 3.0 to 10.0 were prepared using sodium dihydrogen phosphate (NaH_2PO_4) and disodium hydrogen phosphate (Na_2HPO_4) to maintain stable pH conditions during the experiments. Ammonium iron(II) sulfate hexahydrate ($(\text{NH}_4)_2\text{Fe}(\text{SO}_4)_2 \cdot 6\text{H}_2\text{O}$) and iron(III) chloride hexahydrate ($\text{FeCl}_3 \cdot 6\text{H}_2\text{O}$), used for magnetic nanoparticle synthesis, were obtained from Merck (Germany). Oleic acid ($\text{C}_{18}\text{H}_{34}\text{O}_2$), used as a surface modifier to increase the hydrophobicity and adsorption efficiency of the nanoparticles, was purchased from Sigma-Aldrich (Product No: CHO18342). Concentrated nitric acid (HNO_3) was used as the eluent in the desorption step. All chemicals used in this study were of analytical reagent grade, and ultrapure water (18.2 M Ω ·cm) was used throughout all procedures.

Apparatus

In this study, a variety of instruments were utilized for precise measurements and sample preparation. Flame atomic absorption spectroscopy (FAAS) measurements were conducted using a PerkinElmer Analyst 400 atomic absorption spectrometer equipped with a Slotted Quartz Tube (SQT) enhancement system. The SQT was mounted directly above the burner head to increase the residence time of the analyte in the optical path, thereby improving sensitivity. A hollow cathode lamp specific for tellurium was used as the radiation source. Fig. 1 shows the slit quartz tube integration of the flame atomic absorption spectrometer.

Samples were introduced using a micro-volume nebulization system attached to a spray chamber. A 200 μL eluate volume, obtained after the extraction process, was injected manually into the nebulizer using a micropipette. This volume was sufficient due to the high sensitivity of the SQT-integrated system. The sample aerosol generated in the nebulizer was carried to the flame via an air-acetylene mixture. Atomized tellurium species were detected by the system's photomultiplier detector after the lamp absorbed radiation.

Additional equipment used included: IKA RCT ST S000 hot plate for sample heating, OHAUS Pioneer PA214C analytical balance for weighing chemicals, Hanna Instruments Edge® HI2020 multiparameter pH meter for pH adjustments, Thermo Scientific Heratherm oven for drying synthesized nanoparticles, ISOLAB Advanced Vortex and Kermanlar mechanical shaker for mixing during extraction steps, Neodymium magnets for rapid and efficient separation of magnetic nanoparticles from solution. All instruments were calibrated and verified for accuracy prior to use in each experiment.

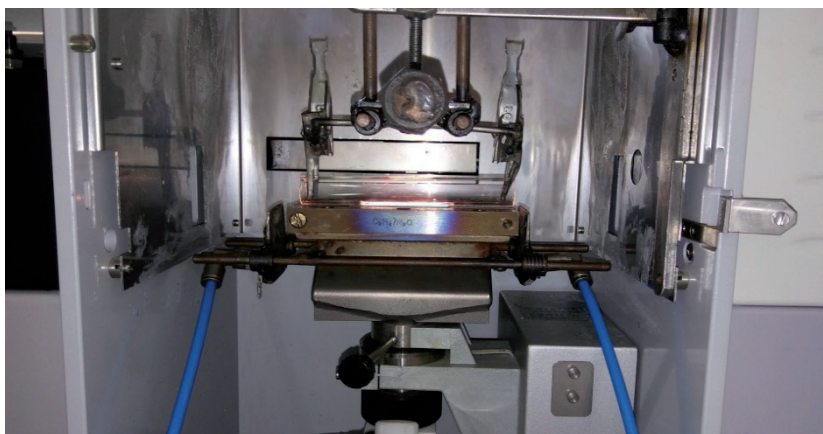


Fig. 1. FAAS (Flame Atomic Absorption Spectroscopy) Instrument with SQT (Slotted Quartz Tube).

Synthesis of Coated Magnetic Nanoparticles

The synthesis of coated magnetic nanoparticles was carried out following the guidelines of a previously published study. The process was as follows: $\text{FeCl}_3 \cdot 6\text{H}_2\text{O}$ (8,109 g) and $(\text{NH}_4)_2\text{FeSO}_4 \cdot 6\text{H}_2\text{O}$ (3,278 g) were placed in a conical flask and then diluted with 100 mL of ultrapure water. Stirred at 900 rpm, it was transferred to a hot plate and heated to 80°C . At this stage, dropwise, 10 mL of 25% NH_3 and 1 mL of oleic acid were added [23]. The synthesized nanoparticle is given in Fig. 2.

Extraction Procedure

50 mg of magnetic nanoparticles (OAMNPs) were weighed and added into a tube containing 30 mL of aqueous tellurium solution. To adjust and stabilize the pH of the solution, 1 mL of phosphate buffer (pH 8.0) was added. The mixture was manually shaken for 45 seconds, followed by vortexing for 30 seconds to ensure homogeneous dispersion of the nanoparticles. Complete dispersion of OAMNPs was visually confirmed before proceeding to the next step.

After adsorption, the tellurium-loaded nanoparticles were collected at the bottom of the tube using a neodymium magnet, and the supernatant was carefully



Fig. 2. Nanoparticles produced.

discarded. The retained particles were then eluted with 200 μL of 7 mol L^{-1} nitric acid (HNO_3). The acid-treated suspension was shaken briefly to ensure desorption and the resulting supernatant containing the desorbed tellurium was collected for analysis. An additional magnetic separation step was performed to remove any residual nanoparticles to avoid clogging the FAAS nebulizer.

Calibration Curve and Limit of Detection

A series of tellurium standard solutions were prepared to construct the calibration curve in the concentration range of 0.05 to 1 mg/L. Each standard solution was subjected to the same extraction and elution procedures described above. The absorbance values were measured using the SQT-FAAS system under optimized conditions. A calibration plot of absorbance versus tellurium concentration was constructed and found to be linear with a correlation coefficient (R^2) of 0.999.

The limit of detection (LOD) and limit of quantification (LOQ) were calculated using the standard deviation (SD) of six replicate measurements of the lowest concentration and the slope (m) of the calibration curve, using the formulas:

$$\text{LOD} = 3 \times \text{SD} / m$$

$$\text{LOQ} = 10 \times \text{SD} / m$$

The LOD and LOQ were determined to be 0.02 $\mu\text{g/L}$ and 0.07 $\mu\text{g/L}$, respectively, confirming the developed method's high sensitivity.

Results and Discussion

Optimization Studies

To ensure high accuracy and precision, extensive optimization studies were performed on the experimental

Table 1. Optimum conditions for method OAMNP-SPME-SQT FAAS.

Parameter	Optimum values
Sample flow rate	4.5 mL min ⁻¹
Acetylene flow rate	15 L h ⁻¹
SQT height	slotted, 5 cm
Buffer solution pH/volume	pH 8, 1 mL
Amount of nanoparticles	50 mg
Mixing type/volume	Hand shake, 2 min
Eluent type/volume	7 M. HNO ₃ /200 μL

parameters affecting the extraction and detection of tellurium. In each optimization step, only one parameter was varied while others were kept constant. Optimum conditions were determined based on the triplicate measurements' highest average absorbance values (Table 1).

Effect of pH and Buffer Volume

Optimal pH is important in studies as it affects the interaction of the coated nanoparticles with the analyte. Therefore, buffer solutions with pH 3.0, 4.0, 5.0, 6.0, 7.0, 8.0, 9.0, and 10.0 were used (Fig. 3). Besides the optimum pH, different amounts of buffer solutions were also examined to see their effect on absorbance. In this

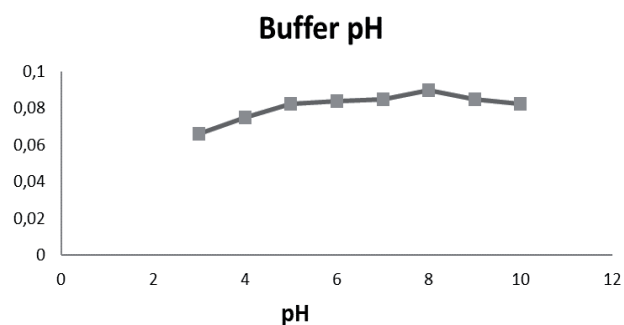


Fig. 3. Optimization of buffer pH.

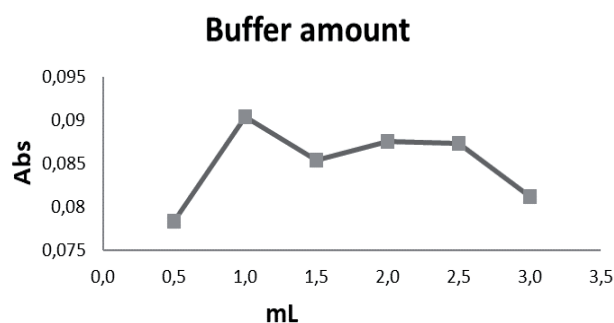


Fig. 4. Optimization of buffer amount.

context, buffer solutions of 0.50, 1, 1.5, 2, 2.5, and 3 mL were tested (Fig. 4). The pH of the sample solution affects the solubility (in water) and adsorption ability of the target metal ions. pH optimization was performed using appropriate buffer solutions in the range of 3-10 to obtain high adsorption efficiency.

Effect of Eluent Type and Volume

Elution efficiency was examined by varying both the molarity (1-10 M) and volume (250-2500 μL) of nitric acid. The optimal elution conditions were found to be 200 μL of 7 mol L⁻¹ HNO₃. This allowed for effective Te(IV) desorption from the nanoparticle surface without dilution effects (Fig. 5 and 6).

Effect of Nanoparticle Amount

The amount of OAMNP used during extraction directly affects the adsorption efficiency. Different masses ranging from 12.5 to 150 mg were tested, and 50 mg was found to be optimal (Fig. 7). Excessive nanoparticle amounts caused aggregation and reduced active surface area, while insufficient amounts limited analyte retention.

Effect of Mixing Method and Time

Determining the ideal interaction time between the adsorbent and analyte is a critical step to achieving

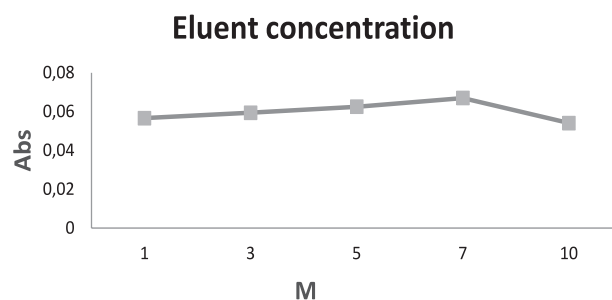


Fig. 5. Optimization of eluent concentration.

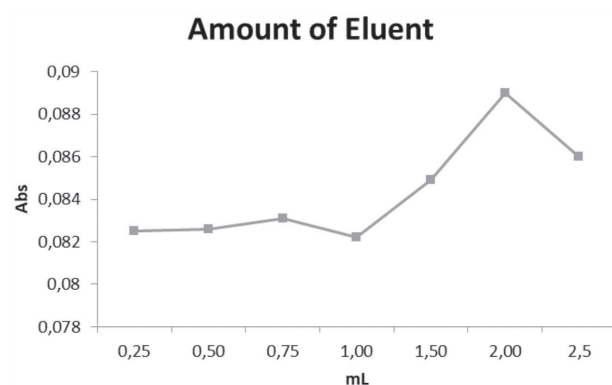


Fig. 6. Optimization of eluent amount.

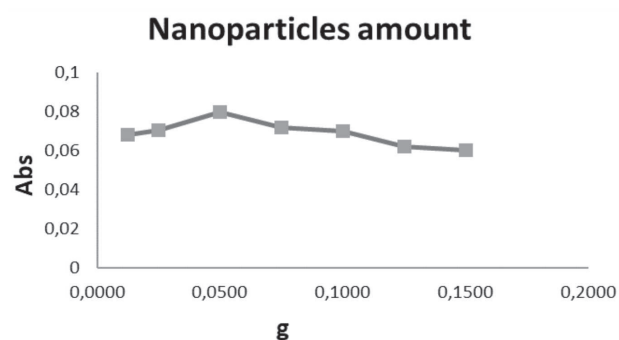


Fig. 7. Optimization of nanoparticle amount.

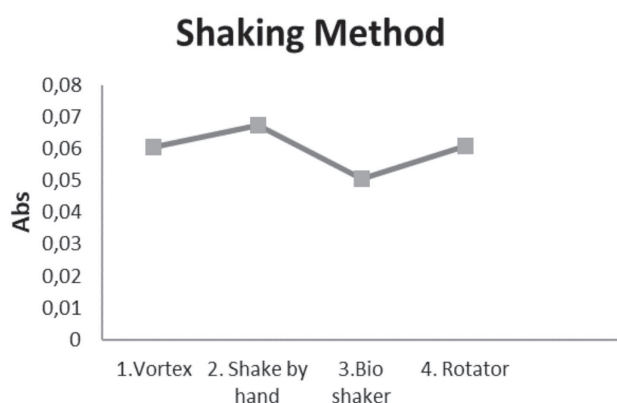


Fig. 8. Optimization of shaking method.

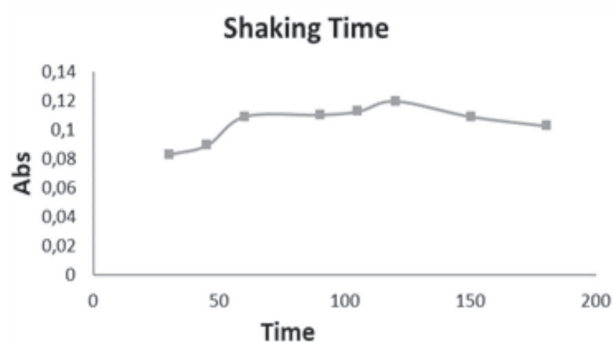


Fig. 9. Optimization of mixing period (mixing period, s).

a complete extraction in SPME studies. For this purpose, different stirring types and times were investigated; manual, ultrasonication, mechanical stirring, and vortex methods were tried (Fig. 8). The vortex mixing method gave the highest absorbance value. As a result of these experiments, 15, 30, 45, 60, 90, 105, 120, 150, and 180 seconds were used (Fig. 9). The agitation mode and time are very important for the maximum transfer of target analytes in solution to the adsorbent surface. The best efficiency was obtained with manual agitation in studies to determine the agitation mode for tellurium. For tellurium, the shaking time was 120 seconds, and it was determined that shaking by hand gave the best results.

Analytical Performance of the Method

Table 2 summarizes the analytical characteristics of the developed method. Combining OAMNP-assisted extraction with SQT-FAAS resulted in superior performance compared to classical techniques.

LOD and LOQ values were dramatically reduced from 1.6 and 5.28 $\mu\text{g/L}$ in classical FAAS to 0.02 and 0.07 $\mu\text{g/L}$ in the OAMNP-SPME-SQT-FAAS method, respectively.

The enrichment factor reached 76.2-fold, confirming the method's capacity for ultra-trace level detection.

The calibration curve demonstrated excellent linearity ($R^2 = 0.999$), and the % RSD values ranged between 2.1% and 4.3%, indicating good repeatability and precision.

Compared to conventional FAAS and even SQT-FAAS alone, the proposed method showed a marked improvement in detection power, selectivity, and operational simplicity. This comparison highlights the advantage of combining nanoparticle-assisted preconcentration with slotted quartz tube enhancement, as it significantly boosts detection power without requiring expensive instrumentation like ICP-MS.

Interference Studies

The potential interferences from commonly coexisting ions were thoroughly evaluated to assess the selectivity of the developed method. Various cations (K^+ , Na^+ , Ca^{2+} , Mg^{2+} , Cu^{2+} , Zn^{2+} , Ni^{2+} , Fe^{3+}) and anions (NH_4^+ , CO_3^{2-} , F^- , Cl^-) were individually added to the tellurium solution at relevant concentrations, as detailed in Table 3. The recovery rates for tellurium ranged between 92% and 105%, indicating that none of the tested species caused significant interference under the optimized conditions.

Special attention was given to Fe^{3+} , which is inherently present in the structure of the magnetic nanoparticles used for extraction. During the desorption process with 7 mol L^{-1} HNO_3 , partial dissolution of Fe^{3+} is possible, raising concerns about potential spectral interference in FAAS measurements. However, experimental results revealed that 100 mg/L of Fe^{3+} had no adverse effect on Te(IV) determination, yielding $102 \pm 4\%$ recovery. This can be attributed to the fact that: Tellurium was measured at 214.3 nm, whereas Fe is typically monitored at 248.3 nm in FAAS, eliminating direct spectral overlap. A secondary magnetic separation step was performed after elution to remove any residual iron-containing particles before the sample was introduced into the nebulizer. Additionally, the system's high selectivity and small injection volume (200 μL) further reduced the likelihood of matrix-related spectral interference.

These findings confirm that the developed OAMNP-SPME-SQT-FAAS method maintains excellent selectivity and is not significantly affected by the presence of common ions, including Fe^{3+} , in the sample matrix.

Table 2. Analytical performance of the studies' systems.

Method	LOD $\mu\text{g L}^{-1}$	LOQ $\mu\text{g L}^{-1}$	%RSD $\mu\text{g L}^{-1}$	Range $\mu\text{g L}^{-1}$	Enhancement in detection power
FAAS	1,6	5,28	3,5	1-10	----
SQT-FAAS	0,9	3,00	2,8	1-10	1,78
OAMNP-SPME-FAAS	0,04	0,13	2,1	0,2-5	40
OAMNP-SPME-SQT-FAAS	0,02	0,07	4,3	0,05-1	76,20

Table 3. The effect of eight cations and four anions on Te (IV) determination.

Interfering ion	Added As	Concentration (mg/L)	Recovery (%)
K^+	KNO_3	3000	94±2
Na^+	NaNO_3	3000	105±1
Ca^{2+}	$\text{Ca}(\text{NO}_3)_2$	500	96±3
Mg^{2+}	$\text{Mg}(\text{NO}_3)_2$	50	98±1
Cu^{2+}	Copper standard for AAS	10	98±2
Zn^{2+}	Zinc standard for AAS	10	92±1
Ni^{2+}	Nickel standard for AAS	50	96±2
Fe^{3+}	Iron standard for AAS	100	102±4
NH_4^+	NH_4NO_3	1000	99±1
CO_3^{2-}	Na_2CO_3	1000	97±3
F^-	NaF	1000	99±2
Cl^-	NaCl	3000	101±1

Table 4. Recovery studies were performed on ice tea samples.

Sample Name	Added (mg/L)	Measured (mg/kg)	Recovery (%)
IceTea1 (A)	--	N.D.	--
	0.25	0.27±0.09	108
	0.50	0.49±0.14	98
	1.00	1.05±0.21	105
IceTea 2 (B)	--	N.D.	--
	0.25	0.23±0.04	92
	0.50	0.51±0.09	102
	1.00	1.07±0.21	107
IceTea 3 (C)	--	N.D.	--
	0.25	0.26±0.02	104
	0.50	0.47±0.14	94
	1.00	0.98±0.21	98

N.D: Not detected.

Recovery Studies on Real Samples

Recovery experiments were performed on cold tea samples from three different brands to evaluate the method's applicability to real matrices. Unspiked samples showed no detectable tellurium, confirming the method's specificity. Spiked samples demonstrated recovery rates between 92% and 108%, with low standard deviations, as shown in Table 4. These results validate the method's accuracy, precision, and suitability for complex beverage matrices.

Summary

The developed OAMNP-SPME-SQT-FAAS method offers a powerful and reliable approach for trace-level tellurium analysis. It provides high sensitivity (LOD: 0.02 µg/L), excellent enrichment (76.2-fold), strong selectivity in the presence of interfering ions, accuracy and reproducibility in real-sample matrices.

This method outperforms many existing FAAS-based techniques and offers a cost-effective, fast, and simple alternative to advanced instrumentation such as ICP-MS or GFAAS, particularly valuable for routine environmental and food sample analysis.

Conclusions

In this study, a novel, sensitive, and cost-effective analytical method was developed for the determination of trace levels of tellurium (Te) in complex matrices using oleic acid-coated magnetic nanoparticles (OAMNPs) coupled with slotted quartz tube-flame atomic absorption spectroscopy (SQT-FAAS). The method was systematically optimized to enhance detection performance and selectivity.

Through detailed optimization, the following optimum conditions were established:

- pH of sample solution: 8.0
- Volume of buffer solution: 1 mL (phosphate buffer)
- Amount of OAMNPs: 50 mg
- Eluent concentration: 7 mol L⁻¹ HNO₃
- Eluent volume: 200 µL
- Mixing method and time: Manual shaking, 120 seconds
- Sample volume: 30 mL
- Detection wavelength: 214.3 nm (Te)

Under these conditions, the method achieved a limit of detection (LOD) of 0.02 µg L⁻¹ and a limit of quantification (LOQ) of 0.07 µg L⁻¹, with a 76.2-fold enhancement in detection power compared to conventional FAAS. The calibration curve demonstrated excellent linearity ($R^2 = 0.999$), and relative standard deviation (RSD) values ranged from 2.1% to 4.3%, indicating strong precision.

The method also showed high selectivity in the presence of common coexisting ions, including Fe³⁺, and exhibited robust performance in real sample

applications, such as cold tea. Recovery studies confirmed the method's accuracy and applicability, with 92% and 108% recoveries.

Overall, the proposed OAMNP-SPME-SQT-FAAS method is:

- Simple in its instrumentation and procedure,
- Highly sensitive and selective for tellurium at ultra-trace levels,
- Economical and practical for routine environmental and food sample analysis.

Its successful integration of nanoparticle-based extraction with enhanced FAAS detection makes it a valuable alternative to more complex and expensive techniques like ICP-MS or GFAAS for tellurium determination in challenging matrices.

Acknowledgments

This research was supported by the Dicle University Scientific Research Projects (DUBAP) Coordinatorship. Project number FEN-22.005, Year 2022.

Conflict of Interest

The authors declare no conflict of interest.

References

1. ÖZBOLAT G., TULI A. Effects of heavy metal toxicity on human health. *Journal of Archive Literature Review*. **25** (4), 502, **2016**.
2. AKDOGAN A., DIVRIKLI U., SOYLAK M., ELCI L. Assessment of heavy metal levels in street dust samples from Denizli, Turkey, and analysis by flame atomic absorption spectrometry. *Spectroscopy*. **37**, 25, **2016**.
3. EDO G.I., SAMUEL P.O., OLONI G.O., EZEKIEL G.O., IKPEKORO V.O., OBASOHAN P., AGBO J.J. Environmental persistence, bioaccumulation and ecotoxicology of heavy metals. *Chemistry and Ecology*. **40** (3), 322, **2024**.
4. O'LEARY R.M. Tellurium and thallium by flame atomic absorption spectrometry. In: ARBOGAST B.F. (Ed.), *Analytical Methods Manual for the Mineral Resource Surveys Program*, U.S. Geological Survey, Open-File Report. **37**, 96, **1996**.
5. THANGAVEL S., DASH K., DHAVILE S., SAHAYAM A.C. Determination of traces of As, B, Bi, Ga, Ge, P, Pb, Sb, Se, Si and Te in high-purity nickel using inductively coupled plasma-optical emission spectrometry (ICP-OES). *Talanta*. **131**, 505, **2015**.
6. SCHRAMEL P., WENDLER I., ANGERER J. The determination of metals in urine samples by inductively coupled plasma-mass spectrometry. *International Archives of Occupational and Environmental Health*. **69** (3), 219, **1997**.
7. DEMIR C., ER E., KARTOGLU O., ATSEVER B., YAGCI N., ONER O., BAKIRDERE S. Preconcentration of tellurium using magnetic hydrogel-assisted dispersive solid-phase extraction and its determination by slotted

- quartz tube-flame atomic absorption spectrophotometry. *Chemical Papers*. **75**, 4261, **2021**.
8. PEDRO J., STRIPEKIS J., BONIVARDI A., TUDINO M. Determination of tellurium at ultra-trace levels in drinking water by on-line solid phase extraction coupled to graphite furnace atomic absorption spectrometer. *Spectrochimica Acta Part B: Atomic Spectroscopy*. **63** (1), 86, **2008**.
 9. LIU N., XU X., WANG Z., WU W., SHEN P., FU J., LI J. Effect of tellurium on sulfide inclusion, microstructure and properties of industrial bars of a medium-carbon microalloyed steel. *Journal of Materials Research and Technology*. **24**, 2226, **2023**.
 10. DAI Y., GUAN J., ZHANG S., PAN S., XIANYU B., GE Z., XU H. Tellurium-containing polymers: recent developments and trends. *Progress in Polymer Science*. **141**, 101678, **2023**.
 11. SHAO L.X., JIANG D.I.A.O., HU R.X., JI C.Q., TAN W.F., LI H.Y., BING X.I.E. Selective reduction separation and recovery of tellurium and bismuth from acidic leaching solution. *Transactions of Nonferrous Metals Society of China*. **33** (2), 596, **2023**.
 12. LIU Y., MA H., LI A., YI X., LIU Y., ZHAN J., ZHOU H. The cryptic step in biogeochemical tellurium (Te) cycle: indirect elementary Te oxidation mediated by manganese-oxidizing bacteria *Bacillus* sp. FF-1. *Environmental Research*. **238** (2), 117212, **2023**.
 13. MEHRABIAN M., NOROOZIAN E., MAGHSOUDI S. Preparation and application of $\text{Fe}_3\text{O}_4@\text{SiO}_2@\text{poly}(\text{o-phenylenediamine})$ nanoparticles as a novel magnetic sorbent for the solid-phase extraction of tellurium in water samples and its determination by ET-AAS. *Microchemical Journal*. **165**, 106104, **2021**.
 14. FAN J., WANG G., LI Q., YANG H., XU S., ZHANG J., WANG R. Extraction of tellurium and high purity bismuth from processing residue of zinc anode slime by sulfation roasting-leaching-electrodeposition process. *Hydrometallurgy*. **194**, 105348, **2020**.
 15. MOCHALOV L., LOGUNOV A., VOROTYNTSEV A., VOROTYNTSEV V., MASHIN A. Purification of tellurium through thermal decomposition of plasma prepared tellurium hydride. *Separation and Purification Technology*. **204**, 276, **2018**.
 16. KRON T., HANSEN C., WERNER E. Renal excretion of tellurium after peroral administration of different forms of tellurium to healthy human volunteers. *Journal of Trace Elements and Electrolytes in Health and Disease*. **5** (4), 239, **1991**.
 17. TAO X., ZHENG Q., ZENG C., POTTER H., ZHANG Z., ELLINGFORD J., ASSENDER H.E. Bi-Sb-Te containing Cu or Ag for sequential roll-to-roll patterned thin-film thermoelectrics. *Nature Communications*. **16**, 196, **2025**.
 18. LIN X., YANG L., JIANG S., CHENG H., ZHANG Y., LI Y., LIU X. Efficient direct formic acid electrocatalysis enabled by rare earth-doped platinum-tellurium heterostructures. *Nature Communications*. **16** (1), 147, **2025**.
 19. ZHOU X., LI J., CHENG Y., WANG H., GAO Y., SUN J., MA C. Selective separation and efficient extraction of tellurium and gold from complex copper anode slime. *Separation and Purification Technology*. **362**, 131625, **2025**.
 20. MISAWA T., KAGAWA T., OHGAMI N., TAZAKI A., OHNUMA S., NAITO H., KATO M. Elevated level of urinary tellurium is a potential risk for increase of blood pressure in humans and mice. *Environment International*. **188**, 108735, **2024**.
 21. VANZAN D.F., GOMA E.P., LOCATELLI F.R., HONORIO T.D.S., FURTADO P.D.S., RODRIGUES C.R., CABRAL L.M. Evaluation of silybin nanoparticles against liver damage in murine schistosomiasis mansoni infection. *Pharmaceutics*. **16** (5), 618, **2024**.
 22. JHA R., HARLOW H., BENAMARA M., MAYANOVIC R.A. On the structural and molecular properties of PEO and PEO-PPG functionalized chitosan nanoparticles for drug delivery. *Bioengineering*. **11** (4), 372, **2024**.
 23. ÇELİK B., AKKAYA E., BAKIRDERE S., AYDIN F. Determination of indium using vortex assisted solid phase microextraction based on oleic acid coated magnetic nanoparticles combined with slotted quartz tube-flame atomic absorption spectrometry. *Microchemical Journal*. **141**, 7, **2018**.